Laser and Particle Beams (2010), *28*, 109–119.
© Cambridge University Press, 2010 0263-0346/10 $20.00
doi:10.1017/S0263034609990668

Laser-induced optical breakdown applied for laser spark ignition

E. SCHWARZ, S. GROSS, B. FISCHER, I. MURI, J. TAUER, H. KOFLER, AND E. WINTNER
Photonics Institute, Vienna University of Technology, Wien, Austria

(RECEIVED 30 August 2009; ACCEPTED 28 November 2009)

Abstract

In the present article, the experimental investigation of optical breakdown induced by ns/mJ pulses at two wavelengths, 1064 nm and 532 nm, in air of atmospheric pressure is reported and discussed. The obtained breakdown thresholds were compared with theory and are in good agreement. The generated plasmas have been characterized by their amount of scattered laser light, energy transmission, and change of the transmitted temporal shape. Laser-induced plasma formation in a gas, in air, also generates an acoustic pressure wave. The acoustic energy is compared to the laser pulse energy and is found to be linearly dependent. Moreover, the frequency distribution of the characteristic acoustic pressure wave was analyzed. The experiments described were accomplished in order to optimize a laser ignition system with regard to efficiency and costs. The laser system employed for these investigations is a compact high peak power, passively Q-switched, longitudinally diode-pumped solid-state laser. Such a "laser spark plug" should replace conventional spark plugs in internal combustion engines because conventional ignition has reached its limits in terms of efficiency and durability. Thereby, a reduction of pollutant emission should also be feasible.

Keywords: Acoustic pressure wave; Laser-induced plasma; Optical breakdown; Q-switched; Scattered laser light

1. INTRODUCTION

Laser technology of modern solid-state lasers has shown a remarkably fast evolution. One innovative and promising application, which only today, after a long chain of laser improvements, has reached the verge of commercial feasibility, is laser-induced ignition of various combustion processes (Lackner, 2008). This means that highly intensive laser pulses in the nanosecond range, generated in a compact, robust and in the future cost-effective source, are focused to a tens-of-micrometers spot size in order to initiate a spark-like plasma, which can lead to ignition of fuel-air mixtures under internal combustion engine conditions[1] or, in the near future, also of liquid propellants in rocket engines.

The physics of breakdown leading to a laser-induced plasma was first investigated by Morgan and Ireland (1973) and Yablonovitch (1974), and well reviewed by Weyl (1989) and Radziemski and Cremers (1989*a*). The two steps leading to optically excited breakdown are, first (Hughes, 1975), the generation of a few free electrons[2] (Tartar *et al*., 2008) *via* linear absorption or thermionic processes of impurities like dust or aerosols[3] (multiphoton absorption, as mentioned in detail later, is considered to be of lesser importance). These electrons serve as initial receptors of energy through three-body collisions with photons and neutrals. Second and most important, avalanche ionization takes place in the focal region. Classically, free electrons are accelerated by the high electric field associated with the optical pulse in the period between collisions (acting also to thermalize the electron energy distribution). This is an effect called inverse bremsstrahlung (IB) (Tauer *et al.*, 2009; Miziolek *et al.*, 2006). As the electron energies grow, even more collisions produce ionization, other electrons, more energy absorption, and an avalanche-like effect occurs. In the following section, the effects that are responsible for the plasma formation process are described in more detail.

The breakdown threshold is usually specified as the minimum irradiance needed to generate visible plasma.

Address correspondence and reprint requests to: Ernst Wintner, Photonics Institute, Vienna University of Technology, Gusshausstrasse 25-29, 1040 Wien, Austria. E-mail: ernst.wintner@tuwien.ac.at

[1] The "Laser Ignition Group" at Photonics Institute has been involved in this field of research for the last 10 years (see the homepage http://info.tuwien.ac.at/Laserzuendung/de).

[2] Simulations showed that even a few hundred in the focal region are sufficient (Tartar *et al.*, 2008).

[3] Fuel/air mixtures of technical purity used in internal combustion engines provide sufficient impurities (according to footnote 3) with plausible certainty.

https://doi.org/10.1017/S0263034609990668 Published online by Cambridge University Press

For Nd:YAG laser radiation ($\lambda = 1064$ nm), the breakdown threshold in air under atmospheric conditions is on the order of several 10^{11} Wcm^{-2} (Lackner, 2008). Following the breakdown, the plasma expands outward in all directions from the focal volume. As it has been reported (Phuoc, 2003; Kopecek, 2004; Bradley *et al.*, 2004), the laser spark expands asymmetrically after the optical breakdown. During the time span between the onset of breakdown and the end of the laser pulse, the plasma front propagates toward the focusing lens more than it does in the opposite direction. The plasma absorbs laser radiation on the lens-oriented side and therefore the increase of plasma size occurs mostly in the direction of the focusing element. In other words, the plasma grows toward the lens and the result is a pear- or cigar-shaped plasma kernel. Figure 1 shows the development of the spatial shape of the plasma kernel in air for pulse energy far above the threshold level *via* its light emission at 310 nm (for more details see figure caption). At such high pulse energies, the kernel lasts for over 180 ns. The loud sound that one can hear after breakdown is caused by the shockwave expelled from the focal volume. In Section 3.2, investigations on the acoustic energy of laser-induced plasma shock waves are discussed.

As mentioned above, applications of laser-induced breakdown include, among others, laser spark ignition of combustible gases (Lee & Knystautas, 1969; Weinberg & Wilson, 1971). The first investigations of laser ignition initially were performed by pulsed ruby lasers. Consequently, studies of ignition were extended into the ultraviolet and infrared and, as a result, new laser ignition mechanisms were discovered. These mechanisms can, in general, be grouped into four categories (Witriol *et al.*, 1990; Ronney, 1994): (1) Thermal ignition, where the combustible gas is heated by the interaction with the laser beam up to the auto-ignition temperature (this type of ignition usually involves infrared wavelengths and continuous wave (cw) lasers); (2) Photochemical ignition, in which the absorption of photons initiates chemical reactions, which lead to the formation of free radicals driving the combustion processes; (3) Non-resonant spark ignition, in which a laser pulse is focused to sufficient irradiance in order to cause dielectric breakdown of the gas; and (4) Resonant spark ignition, in which a single- or multiphoton resonance is exploited to intensify the initial processes of optical breakdown. A thorough review of these four mechanisms is given in the article by Ronney (1994). Laser spark ignition has been extensively investigated at Vienna University of Technology by the "Laser Ignition Group" (Kopecek *et al.*, 2003; Weinrotter, 2006; Kofler, 2005; Tauer, 2006; Schwarz, 2008). Based on this research work, a laser spark plug for engine ignition was developed by Kofler *et al.* (2007). The laser system is a compact high peak power, passively Q-switched, longitudinally diode-pumped solid-state laser.

Generally, laser ignition systems offer the following essential advantages (Lackner, 2008; Tauer, 2006; Kofler *et al.*, 2007; Miziolek *et al.*, 2006): (1) The free choice of focus of the laser beam, which allows creating the ignition plasma at an arbitrary location. This enables ignition in areas of ideal mixture ratio, which in turn allows reducing the plasma energy compared to electrical spark ignition. (2) The probability to ignite leaner mixtures is higher. As a consequence of the high leanness of the mixtures, the flame temperature is lowered and hence also the NO_x emissions (NO and NO_2 are especially produced during combustion at high temperatures), whereas the efficiency of the engine can be increased simultaneously. (3) There are no quenching effects on the developing flame kernel due to the absence of spark plug electrodes. (4) The laser permits ignition at higher pressure. In contrast to electric spark ignition, the required pulse energy for plasma formation decreases with increasing pressure. (5) For electric spark ignition, the spark voltage has to be raised with increasing pressure, which causes stronger erosion of the electrodes. Laser ignition systems do not require electrodes; hence maintenance intervals of a laser ignition system are expected to be significantly longer than those of a spark plug system. (6) Not only small chambers but also large rocket engine chambers could be ignited on the same basis. The use of complex igniter-torches would not be necessary anymore. (6) The long lifetime of laser diodes in the range of 1 gigashot (10^9 shots), which corresponds to an operating time of $>20\,000$ h,[4] would qualify the laser system for long duration application in satellites as well as in reusable and re-ignitable rocket engines.

The laser-ignition system mentioned above is mounted directly on the cylinder head in a similar way to a conventional spark plug. An external laser diode operates as the optical power supply where the pump beam propagates over a step-index fiber. Since the laser spark plug should be mounted on the cylinder head, like an electric spark plug, the requirements on the laser spark plug are primarily robustness and compactness. No adequate laser system with the necessary specification is available on the market at the current time. Therefore, the "Laser Ignition Group" had to design an ignition laser, delivering ns-pulses in the energy range beyond 10 mJ.

2. BASICS OF PLASMA FORMATION AND MINIMUM IGNITION ENERGY

2.1. Basics of Plasma Formation

Plasma employed for the initiation of combustion processes is generated by a tightly focused pulsed laser beam. For most gases at atmospheric conditions, the required intensity I_{thr} in the focal region for plasma generation is typically on the order of 10^{10} to several 10^{11} W/cm^2.

Plasma formation indispensably requires some initial free electrons in the focus of the laser beam. These charged particles gain energy through the absorption of photons (IB),

[4] Jenoptik quasi-cw laser diode on the basis of 12.5 Hz.

https://doi.org/10.1017/S0263034609990668 Published online by Cambridge University Press

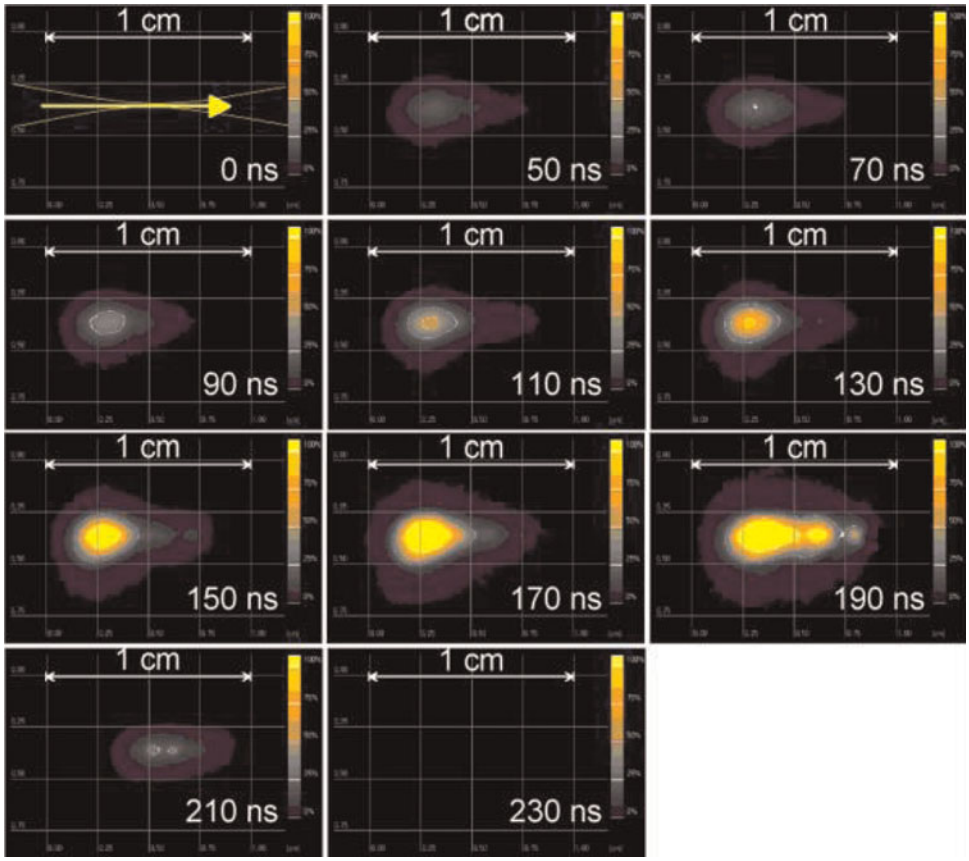


Fig. 1. (Color online) Typical temporal development of a plasma spark in air represented by its emission at 310 nm (corresponding to T ≈ 9000 K). Laser pulse energy $E_p = 230$ mJ; camera exposure time $t_{exp} = 3$ ns; $\lambda = 1064$ nm; $\tau_p = 9$ ns; atmospheric pressure; room temperature; focusing optics $f = 150$ mm, NA = 0.032. Laser light absorption by plasma takes place in the left region of the focus and therefore the plasma expands towards the lens (Kopecek, 2004).

yielding substantial acceleration of them. These accelerated electrons with high probability collide with neutral atoms and ionize them according to the reaction

$$e^- + M \rightarrow 2e^- + M^+ \tag{1}$$

where e^- represents the free electrons and M and M^+ are the neutral and ionized atoms or molecules. This effect is known as the cascade breakdown, where the number of electrons $N_e(t)$ increases exponentially with time (Bäuerle, 2000)

$$N_e = N_{e,0} \exp\left(\frac{t}{\tau_e}\right), \tag{2}$$

where $N_{e,0}$ is the starting electron density and τ_e is a time constant depending on intensity I and diffusion loss. In a more accurate description, the time constant can be written as

$$\tau_e = \left[v_d \left(\frac{I}{I_{thr}} - 1 \right) \right]^{-1} \tag{3}$$

In this equation, v_d represents the diffusion rate of electrons escaping from the plasma per vapor plume. From Eq. (3) it is obvious that high intensities imply a fast growth of the number of free electrons. Considering temporal domains on the order of the pulse length, the time which will elapse until the optical breakdown can occur is closely linked to the time constant defined in Eq. (3). A more detailed discussion of the electron growth rate including all relevant mechanisms of ionization, recombination and diffusion, can be found (Phuoc, 2003; Bäuerle, 2000; Radziemski & Cremers, 1989*b*; Raizer, 1991).

The wavelength $\lambda = 1064$ nm and its second harmonic, $\lambda = 532$ nm, employed in most cases of laser-induced ignition, are not absorbed by the gases (O_2, N_2, CH_4, n-heptane, gasoline, etc.) used for ignition in internal combustion engines. Laser-induced breakdown based on wavelengths not corresponding to any absorption line of the medium is denoted as non-resonant breakdown, which we consider to be the most appropriate mechanism for ignition. Besides non-resonant breakdown, as mentioned before, several other ignition mechanisms exist such as thermal initiation, resonant breakdown, and photochemical ignition (Ronney, 1994). The presence of initial electrons in the focal volume is a necessary condition for the electron density growth. Impurities, like aerosol particles, dust or

https://doi.org/10.1017/S0263034609990668 Published online by Cambridge University Press

vapor in the focus can be the source of some initial electrons. Such particles typically have a low ionization potential (<1 eV) and, therefore, can be ionized resonantly by the laser radiation (e.g., Nd:YAG) or thermionically due to absorptive heating.

Another mechanism describing electron generation and growth is multiphoton ionization (MPI), involving the simultaneous absorption of a sufficient number m of photons by an atom or molecule causing its ionization. This process is described by

$$M + m\hbar\omega \rightarrow e^- + M^+ \tag{4}$$

where m is the number of photons and $E_p = \hbar\omega$ is the photon energy. The ionization energy for gaseous oxygen or gaseous methane is on the order of 12 eV. In the case of Nd:YAG laser radiation with $E_p = 1.17$ eV, more than 10 photons would be necessary for direct ionization. However, MPI is important only at very short wavelength ($\lambda < 1$ μm) or at very low pressures ($p < 10$ mbar), where collision effects are negligible (Phuoc, 2006, 2000). This can be understood insofar that the electron cascade process depends strongly on pressure p while MPI is influenced only slightly by p. Consequently, at very low p MPI becomes the dominating breakdown mechanism given the laser intensity is high enough. At higher pressures ($p > 100$ mbar) and longer wavelengths ($\lambda > 1$ μm), the electron cascade process usually dominates the gas breakdown.

Optical properties of plasma depend primarily on the degree of ionization $\xi = N_e/N_g$ where N_g is the atom/molecule density. In dynamic equilibrium, where the rate of generation is equal to the rate of recombination, ξ is given by the Saha equation (Bäuerle, 2000). Considering focused and/or pulsed laser light, diffusion of electrons out of the vapor/plasma plume and plasma absorption have to be taken into account. For low degrees of ionization, typically $\xi \leq 10^{-2}$, the absorption coefficient can be derived from the linear oscillator model (Drude theory) (Bäuerle, 2000; Reider, 2004). With moderately increasing ionization the Kramers-Unsöld equation can be applied, while for a high degree of ionization $\xi \approx 1$ IB becomes dominant. According to the Drude theory, the absorption coefficient is given by

$$\alpha_p \approx \frac{\omega_p^2 \omega_c}{c\omega^2} \propto \lambda^2 \tag{5}$$

where ω_p is the plasma and ω_c is the collision frequency (Bäuerle, 2000). For plasmas with a low degree of ionization, collisions between electrons and neutral atoms or molecules are relevant, while for the regime $\xi = 1$, ion-electron and electron-electron collisions become more important. An exact description of all contributing processes, however, is very complicated. The most general description of transport processes of atoms, molecules, or charged particles in plasmas is given by the Boltzmann and Fokker-Planck equations (Raizer, 1991; Landau & Lifschitz, 1979; Griem, 1997). A detailed discussion about the origin of the specific processes of plasma formation would go beyond the scope of this work. For the regime of IB, the absorption coefficient can be described, according to (Bäuerle, 2000), by

$$\alpha_{IB} \approx C\lambda^3 \frac{Z^2 N_i N_e}{T_p^{1/2}} \left[1 - \exp\left(-\frac{\hbar\omega}{k_B T_p}\right)\right], \tag{6}$$

where C denotes a constant, T_p is the plasma temperature, Z is the average ion charge, and k_B is the Boltzmann constant. For infrared ($\lambda > 3$ μm) radiation, $<< k_B T_p$ and, consequently, the exponential function in Eq. (6) can be expanded into a Taylor series. In this case, one receives a result similar to Drude's formula in Eq. (5). Therefore, the λ^3-dependence becomes important in the near infrared ($0.75 > \lambda > 3$ μm) region. Other references (Griem, 1997) yielded similar results, where the absorption coefficient also shows a λ^3-dependence. Therefore, the plasma resulting from the electron avalanche process is heated up by absorbing laser radiation. The absorption coefficient depends on the wavelength, according a potential function between λ^2 and λ^3. The longer the wavelength is, the greater the plasma absorption. This finding is of relevance when considering the behavior of plasma transmission. When the plasma state is formed, laser radiation is absorbed by the plasma plume. Before the plasma plume is formed, the laser light just passes through without absorption, which has to be treated as a loss. Such aspects are important, since the laser energy should be kept as low as possible and thus also the costs of the igniting laser spark plug providing the energy (see Section 3.1).

2.2. Minimum Ignition Energy

For successful combustion initiation, a certain amount of ignition energy is required. This energy is called minimum ignition energy (MIE), and its amount depends on the specific ignition conditions. The flame front of a self-propagating flame has a characteristic thickness d_F that is a result of the balance between heat conduction and diffusion losses to the unburned mixture, on the one hand, and the heat release by the chemical reaction, on the other. Thus, the input energy of the ignition source must exceed MIE to raise a sphere of gas with a radius δ_F to a characteristic flame kernel temperature *Tf*. Therefore the radius δ_F is also called the minimum kernel radius (Williams, 1985).

For deflagrative combustion, MIE can be roughly estimated by

$$MIE \approx \frac{4 \cdot \pi \cdot \delta_F^3}{3} \cdot \rho_F \cdot c_p \cdot (T_F - T_{gas}), \tag{7}$$

where ρ_F is the density in the volume behind the flame front, c_p is the specific heat, T_F is the ignition temperature, and T_{gas}

https://doi.org/10.1017/S0263034609990668 Published online by Cambridge University Press

is the ambient gas temperature. The minimum radius δ_F is estimated by

$$\delta_F \approx \frac{\kappa}{\rho_0 \cdot c_p \cdot v_f}, \tag{8}$$

where κ is average heat conductivity of the gas mixture, ρ_0 is the ambient gas density, and v_f is the propagation velocity of the flame front, which strongly depends on the air-equivalence ratio λ_{equ} characterizing mixtures of fuel and air. Three different fields of λ_{equ} can be defined: Mixtures with values of $\lambda_{equ} < 1$ contain more fuel than oxygen and, hence, they are called rich mixtures. The stoichiometric composition is defined by a value of $\lambda_{equ} = 1$, and mixtures in the range of $\lambda_{equ} > 1$ are called lean mixtures.

Figure 2 shows the MIE dependence of a methane/air mixture ignited by an electric spark for different equivalence ratios at 1 bar and 20°C. The lowest MIE occurs at equivalence ratios between $\lambda_{equ} = 1–1.2$ having approximate values of 0.4 mJ (Lewis & Elbe, 1987) and $\delta_F \approx 0.3$ mm. However, with increasing distance from that point MIE increases exponentially. Already at $\lambda_{equ} = 1.7$, MIE ≈ 4 mJ with a measured $\delta_F \approx 1.1$ mm (Williams, 1985) is needed to ignite the mixture.

In contrast to electric spark ignition, the MIE dependence of a laser-ignited methane-air mixture is depicted in Figure 3 for different initial temperatures (gas temperature after compression) (Weinrotter *et al.*, 2005). MIE for a certain equivalence ratio decreases with the ignition temperature due to thermal broadening of the flammability limits.

In order to obtain laser plasma in a gas, certain breakdown intensity must be exceeded. This requires a laser pulse delivering minimum plasma energy E_{pl} depending on pulse duration, focusing optics, gas density and laser wavelength. For stoichiometric mixtures E_{pl} usually exceeds MIE as it can be seen in the diagram.

While turbulences in the combustion chamber have no effect on the minimum plasma energy (MPE), because the time scale of turbulence (several 100 μs to 1 ms) is considerably larger than the time scale of a laser spark (in the ns range), the influence on MIE cannot be neglected.

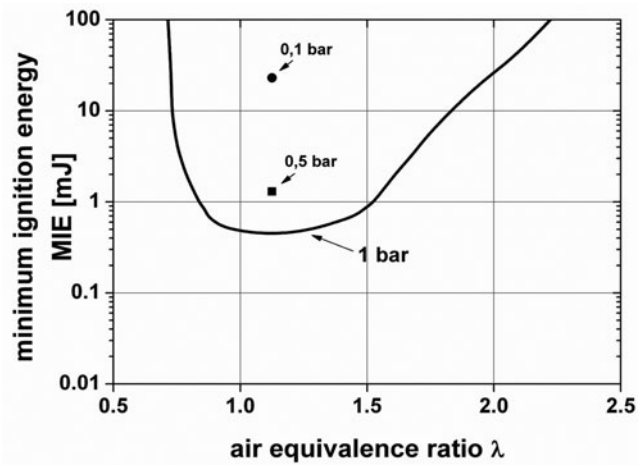


Fig. 2. Minimum electrical spark ignition energies for a methane-air mixture at 20°C for different pressures.

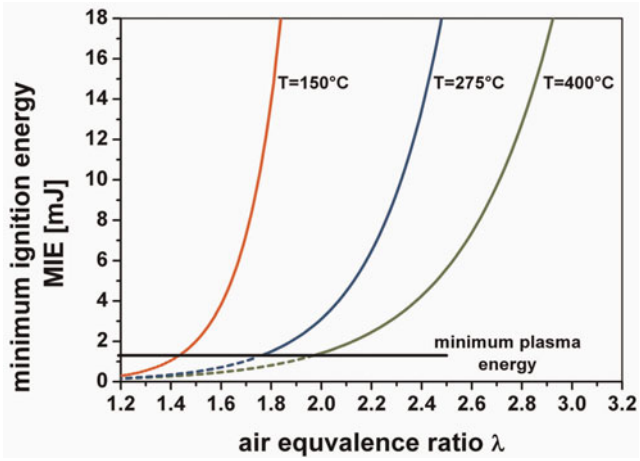


Fig. 3. (Color online) MIE at different equivalence ratios λ_{equ} and three different ignition temperatures. The MPE is mainly defined by the ignition pressure (20 bar) and the focal volume.

Increasing the flow velocity in the ignition volume increases the MIE because the flow stretches the spark downstream. This, in turn, leads to an increase of the spark path length and hence causes the energy input to be distributed over a much larger volume. Consequently, the achievable temperature is reduced. If the flow is turbulent, there is an additional heat loss mechanism off the kernel due to the higher strain and hence larger MIE is needed. Detailed information on this topic can be found (Bradley *et al.*, 2004; Glassmann, 1987; Mastorakos, 2009; Huang *et al.*, 2007).

3. EXPERIMENTS

The following section is a description of two investigations concerning laser-induced optical breakdown. First, experimental results of two-color laser ignition are presented for the first time. Two-color laser ignition takes advantage of the fact that a shorter wavelength can be focused to a smaller focal spot size. Some consequences which result from that are discussed in Sections 3 and 3.1. Part of the incident laser pulse energy is converted into acoustic energy after plasma generation. Hence, the energy of an acoustic shock wave, induced by the laser-optical breakdown in air, was measured. Results are described in Section 3.3.

3.1. Two-Color Laser Ignition

As mentioned before, laser-induced ignition offers numerous advantages, e.g., in case of internal combustion engines, such as reduction of pollutant emissions and increase of engine efficiency. For the commercial implementation, an important aspect of laser ignition is the efficiency of the ignition system, which also defines its cost. By reducing the

https://doi.org/10.1017/S0263034609990668 Published online by Cambridge University Press

required pulse energy for ignition and consequently the pump power, the overall efficiency of the laser ignition system can be increased. A favorable side aspect of lowered pump power is the decreasing thermal load of the laser crystal. This leads to a better beam quality and hence the laser pulse can be focused to a smaller focal spot size. A smaller spot implies larger intensity and therefore earlier breakdown of the combustible fuel-air mixture. A pulse energy reduction can be attained by using a smaller wavelength for ignition, since the focal spot size of a laser pulse resulting from focusing with a lens scales linearly with its wavelength. Therefore, the obtained intensity scales quadratically with the wavelength, however, also plasma absorption is lower at shorter wavelengths, resulting in a lower plasma temperature, since less energy is deposited in the plasma plume. To circumvent this dilemma, the idea of two-color laser ignition was conceived. It should combine the better focusability of the lower wavelength radiation and the higher plasma absorption of the long wavelength radiation. From the ideal case, there should be a temporal delay between the two pulses. The longer wavelength pulse should be delayed with respect to the short wavelength. Thus, early breakdown would be achieved by the short wavelength radiation and almost the whole long wavelength radiation could be absorbed within the already emerged plasma. In order to obtain two-color radiation second harmonic generation can be employed. Therefore, a commercial Q-switched 1064 nm Nd:YAG laser (Quantel Brilliant, pulse length 5 ns, maximum energy 365 mJ) was frequency-doubled *via* a KTP crystal. The breakdown threshold difference between 532 nm and 1064 nm radiation was experimentally determined (Gross, 2008). The plasmas were analyzed and compared for their energy content and temporal transmission evolution. The amount of scattered laser light was measured with an integrated sphere and the scattered intensity is angularly resolved.

3.2. Comparison of Plasma Threshold at 1064 nm and 532 nm

The threshold intensity I_{thr} for cascade breakdown has a significant wavelength λ and pressure p dependency

$$I_{thr} \propto \frac{1}{p^n}\frac{1}{\lambda^2} \tag{9}$$

If the laser pulse is short, the diffusion loss is negligible, and hence the threshold is proportional to p^{-1} ($n = 1$), and consequently decreases as the gas pressure increases. If, however, the pulse is long (>1 ns) then the diffusion loss of the electrons in the plasma plume becomes important. In this case, the threshold is proportional to p^{-2} ($n = 2$) (Bradley *et al.*, 2004; Phuoc, 2006). However, there is no sharp boundary and the product of pulse length and pressure defines the limits (Morgan, 1975).

For a laser pulse length of 5 ns and pressures from 1 bar up to 60 bar, our experimental results show a p^{-k} $k \in [0,1]$ dependency. The observed pressure dependency of the MPE indicates that electron cascade breakdown and not MPI (Barnes *et al.*, 1990) is the dominant mechanism ($1/p^{0.49}$ at 1064 nm, $1/p^{0.42}$ at 532 nm) at both wavelengths. For MPI, the exponent would be ≈ -0.1 and ≈ -0.2, respectively. The slight difference in pressure dependency can be attributed to diffusion losses, which are more dominant at 532 nm, due to the smaller focal volume (Phuoc, 2006).

Nevertheless, a shorter wavelength can be focused to a smaller spot size (Bäuerle, 2000)

$$2w_0 \approx \frac{4}{\pi}\lambda\frac{f}{D_0}, \tag{10}$$

where $2w_0$ is the diameter of the focal spot, f is the focal length of the lens, and D_0 the beam diameter at the lens surface. Since the intensity is inversely proportional to the square of the focal diameter, the larger threshold of 532 nm radiation can be compensated.

For threshold comparison of the two wavelengths $\lambda =$ 1064 nm and $\lambda = 532$ nm, a plano-convex spherical lens with $f = 75$ mm was used to focus the laser beam. In order to obtain equal focal spot sizes (Fig. 4b) according to Eq. (10), the beam diameter of 532 nm was decreased by a factor of two by introducing an additional demagnifying 2:1 telescope into the beam. The profiles of the fundamental laser beam and of its second harmonic at the lens are illustrated in Figure 5. In Table 1, the measured beam diameters D_0 on the lens surface, the calculated focal spot radii w_0 and the calculated focal area are listed.

As illustrated in Figure 6, the MPE necessary for generating an optical spark at atmospheric pressure at 532 nm is 37% lower than at 1064 nm, due to tighter focusing of the 532-nm radiation. For increasing pressure, the difference in MPE at 532 nm to MPE at 1064 nm drops to 30%. This decrease in the difference might be attributed to the way the 532 nm pulse energy was adjusted. The change of the laser pulse energy was obtained by adjusting the pulse energy of the fundamental wave. A change in the fundamental wave's energy leads to a change of the conversion efficiency, which changes the pulse width of the second harmonic wave. Therefore, by decreasing the pulse energy of the fundamental, the conversion efficiency becomes lower.

For an equal spot size, the required minimum energy for optical breakdown at 532 nm is 60% higher than at 1064 nm. In Figure 7, the threshold intensities of 1064 nm and 532 nm are compared with respect to pressure. Note that the threshold intensity at 532 nm is 2.7 times higher than at 1064 nm, where, according to Eq. (9), there should theoretically be a factor of 4 increase.

Nevertheless, due to the better focusability of the green second harmonic generation radiation to smaller focal spot sizes, less laser pulse energy is needed to achieve optical breakdown, compared to the infrared light.

https://doi.org/10.1017/S0263034609990668 Published online by Cambridge University Press

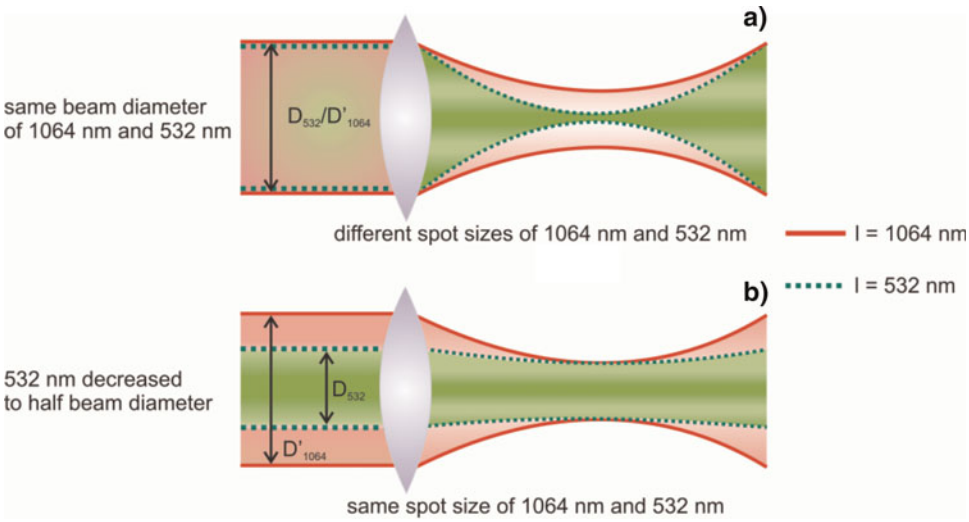


Fig. 4. (Color online) Schematic drawing of the focal spot sizes. To determine the difference in threshold intensity the better focusability of 532 nm had to be compensated by decreasing the beam diameter by a factor of two. (**a**) Both wavelengths have the same beam diameter on the focusing lens, but different focal spot sizes. (**b**) To get the same focal spot size for both wavelengths the beam diameter of the wavelength 532 nm was decreased by a factor of 2.

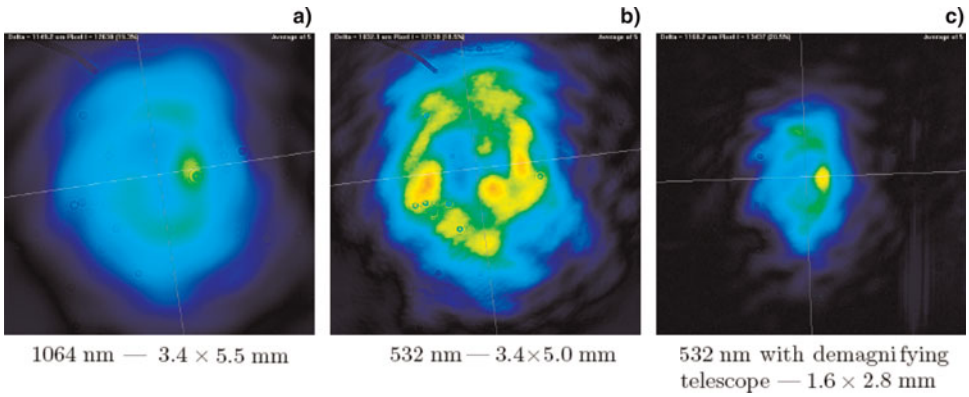


Fig. 5. (Color online) Beam profiles at the $f = 75$ mm lens surface. The profiles were recorded with a WinCamD beam profiler (ISO 11146).

3.3. Plasma Transmission and Scattering at 1064 nm and 532 nm

Plasma transmission and scattering measurements were conducted in the laboratory at atmospheric pressure using a lens with an effective focal length of 40 mm. The transmitted energy was captured with a pyroelectric detector, which was placed behind the plasma. Figure 8 depicts the plasma transmission dependence on the pulse energy for 1064 nm and 532 nm. Even if 532 nm features a lower MPE, at approximately 10 mJ pulse energy, more energy can be deposited into the plasma by infrared radiation. As mentioned in Section 1, the absorption coefficient depends on the wavelength on the order of λ^2 and λ^3. Experimentally, the observation was made the longer the wavelength is, the greater the plasma absorption efficiency. Figure 8 shows that the laser pulse energy for plasma formation at 532 nm (2.5 mJ) is half the energy required for plasma generation at 1064 nm (4.8 mJ). This effect can be attributed to the two-fold increase in focusability of the shorter wavelength.

For plasma scattering, an integrating sphere, as depicted in Figure 9, was used to capture the amount of scattered energy. The loss of energy by plasma transmission, due to its delayed buildup, is much higher than by plasma scattering. While

Table 1. *Spot radii w_0 and focal spot areas were calculated according to Eq. (10) by using the measured beam diameters D_0 shown in Figure 5*

	$D_{0,x}$ [mm]	$D_{0,y}$ [mm]	$w_{0,x}$ [μm]	$w_{0,y}$ [μm]	Focal spot area [μm^2]
1064 nm	3.4	5.5	14.94	9.24	433.68
532 nm	3.4	5.0	7.47	5.08	119.22
532 nm (corr[5])	1.6	2.8	15.86	9.07	451.92

https://doi.org/10.1017/S0263034609990668 Published online by Cambridge University Press

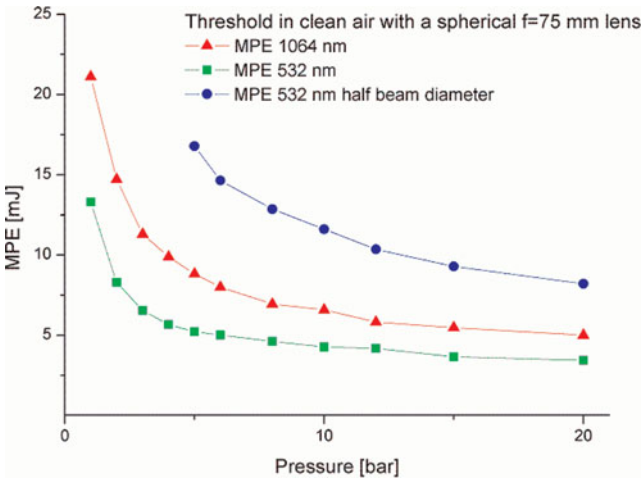


Fig. 6. (Color online) MPE for breakdown in clean air *vs*. pressure for 1064, 532 nm radiation and 532 nm at half beam radius for achieving the same focal area. For increasing pressure, the probability of ionization by collision increases, due to the higher collision frequency ω_c.

transmissions are on the order of 30−40%, the scattered amount is, as shown in Figure 10, far below 5%. There was an observable continuous rise of the scattered fraction with increasing pulse energy.

3.4. Acoustic Energy of Laser-Induced Plasma Shock Waves in Air

For a comprehensive description of the optical breakdown process, detailed knowledge of the particular energy conversion mechanisms is necessary. One part of the overall energy of laser-generated plasma in air dissipates into the acoustic emission. Although the generation of acoustic pulses in liquids or solids is well known (Vogel, 1999; Dewhurst, 1982), little work on plasma acoustics in air is in the literature.

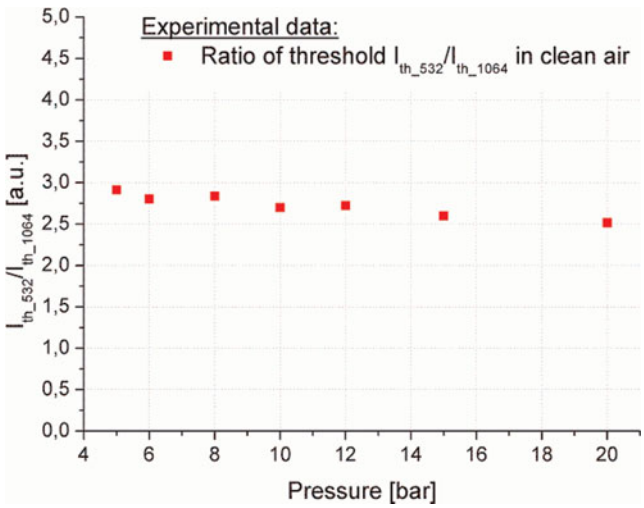


Fig. 7. (Color online) Threshold intensity comparison between 1064 nm and 532 nm radiation respectively. The threshold intensity is by a factor of approximately 2.7 larger at 532 nm than at 1064 nm.

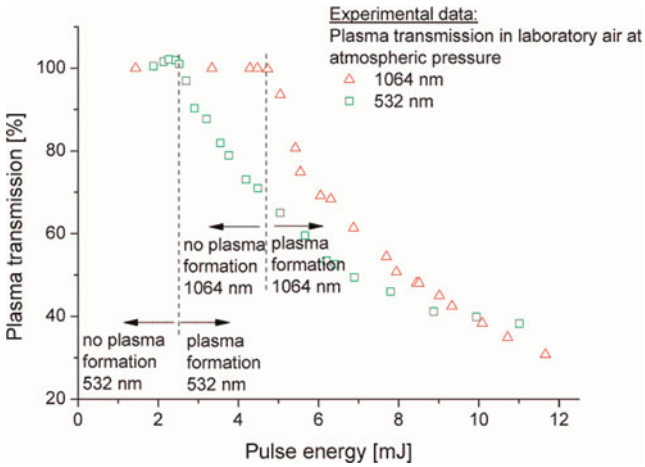


Fig. 8. (Color online) Relative plasma transmission vs. pulse energy for 1064 nm and 532 nm radiation (MPE at 1064 nm: 4.8 mJ; MPE at 532 nm: 2.5 mJ).

The sound emission of laser-induced plasma originates in the thermal supersonic expansion of the heated focal volume, which can be seen in Figure 11. The thin ring around the plasma plume shows the expanding shockwave 2.5 μs after breakdown. Initial expansion speeds on a ns timescale are on the order of 10 km/s, however, the speed drops rapidly with evolving time after the laser pulse, so that after some hundreds of μs the regular velocity of sound propagation (340 m/s) is reached (Sobral, 2000).

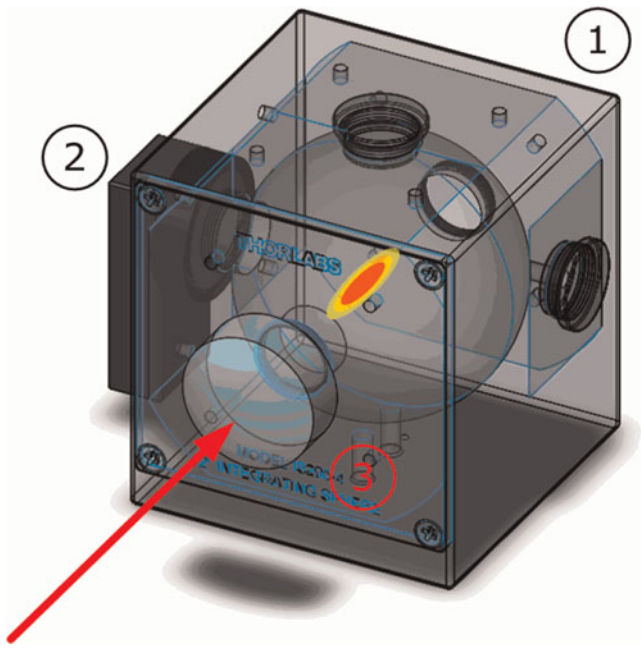


Fig. 9. (Color online) Experimental setup of plasma scattering investigations. (**1**) 2" integrated sphere (Thorlabs IS200-4); (**2**) Ophir PD300-3W photodiode power detector with laser line filter 1064/532 nm; (**3**) Achromat $f = 40$ mm (Edmund Optics NT49-354).

https://doi.org/10.1017/S0263034609990668 Published online by Cambridge University Press

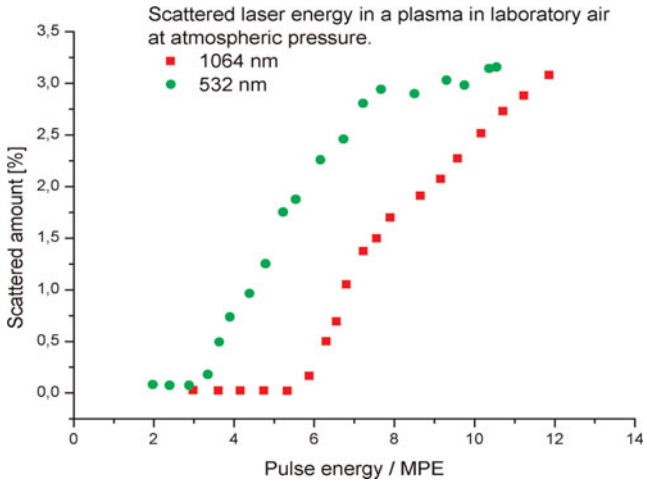


Fig. 10. (Color online) Relative part of plasma scattering vs. pulse energy. At the laser pulse energy of 10 mJ, approximately 3% of the incident energy is lost by plasma scattering.

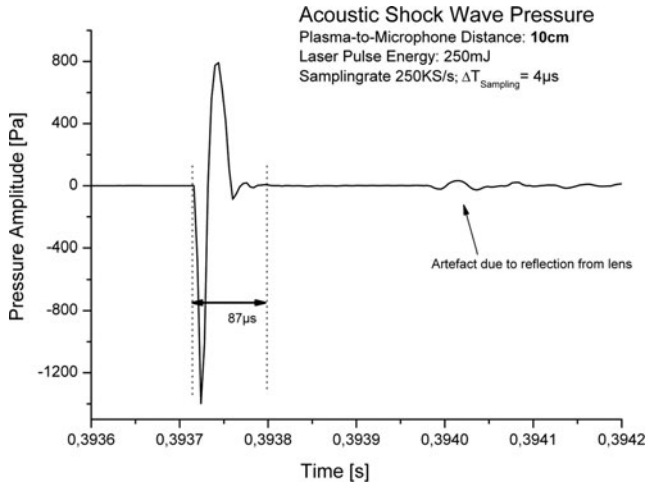


Fig. 12. Acoustic pressure shock wave measured with condenser microphone; the signal is inverted in the amplifier.

3.5. Experimental Setup and Results

As a beam source, the same actively Q-switched flash lamp-pumped Nd:YAG laser with a pulse duration of 5 ns was used as before. The plasma was generated in air under normal conditions. The laser pulse energy was varied between 7.5 mJ (being the threshold energy for plasma formation) up to 250 mJ. Acoustic pressure changes were measured at distances between 8 cm and 140 cm from the plasma spark. Measurements were carried out using a one-quarter inch free field condenser microphone, having a linear frequency response (± 2 dB) between 2 Hz up to 100 kHz, and an upper limit of dynamic range of 166 dB rel. 20 µPa. The signal was amplified and converted with a 16 Bit 250 KS/s A/D converter for analysis in LabView software. Figure 12 depicts an acoustic pressure shock wave.

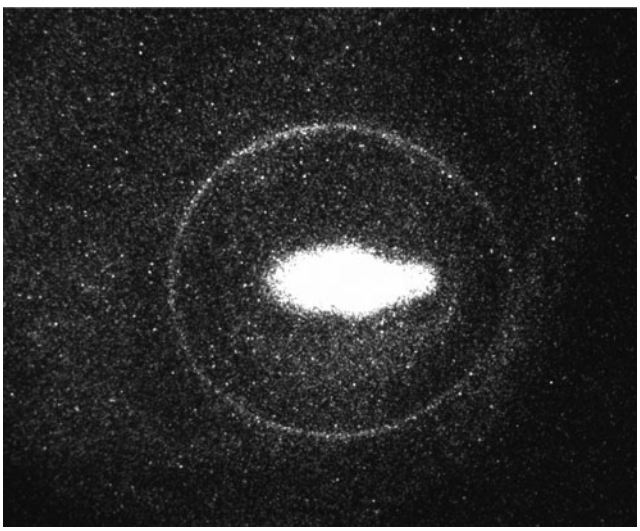


Fig. 11. Schlieren photography of plasma plume with detaching shockwave 2.5 µs after breakdown (laser beam entering from left side). Air, 1 bar, 50 mJ laser pulse energy at 1064 nm, 6 ns duration (Lackner, 2008).

While the acoustic pressure $\tilde{p}$ is a parameter easily accessible to measurement, acoustic energy is not. Acoustic intensity is the product of pressure times particle velocity v, the latter being a parameter difficult to measure. Therefore, the relationship $v = \tilde{P}/Z$ has been used, where Z is the characteristic impedance of the sound propagating medium ($Z_{air} = 408\ \mathrm{Ns/m^3}$ at normal conditions). However, this relationship only holds true in the far field of a spherical wave, i.e., $k \cdot r > 1$, where r is the distance and k is the wave number. Acoustic energy is therefore given by

$$E_{Acoustic} = \frac{4\pi r^2}{Z} \int \tilde{p}^2 dt. \tag{11}$$

The distance $r = 0.25$ m has been chosen to minimize air absorption, which can be substantial for high frequencies (as much as 200 dB per 100 m at 100 kHz (Fahy, 2001)), and, at the same time, the far field condition is fulfilled for frequencies above 250 Hz. Laser-induced plasmas give rise to high pressure shock waves on the order of 100 Pa at a distance of 1 m for a 250 mJ laser pulse. This corresponds to a sound pressure peak level of 134 dB rel. 20 µPa. Fourier transforms of pressure waves indicate that the peak frequency tends to shift towards lower frequency with higher pulse energy (Fig. 13). While the peak frequency of the 250 mJ laser pulse lies at around 20 kHz, it shifts to approximately 50 kHz for the 7.5 mJ pulse. The acoustic energy depends approximately linearly on laser pulse energy. Conversion efficiency from the laser pulse energy (not to be confused with plasma energy) to acoustic energy in the measured frequency range is found to be approximately 2% (Fig. 14).

https://doi.org/10.1017/S0263034609990668 Published online by Cambridge University Press

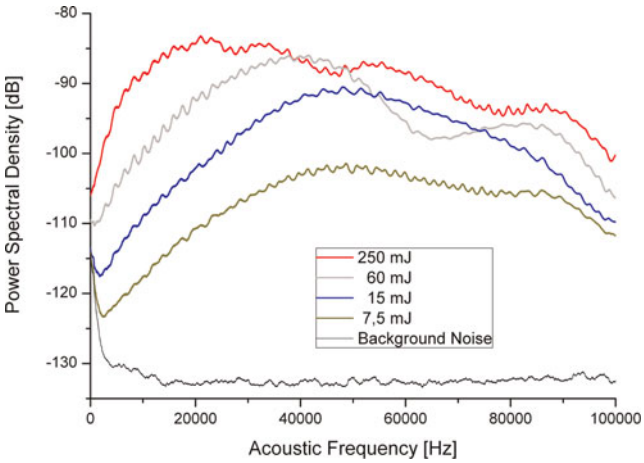


Fig. 13. (Color online) FFT frequency spectrum of the acoustic shock wave at different laser energies. The plasma-to-microphone distance is 0.25 m.

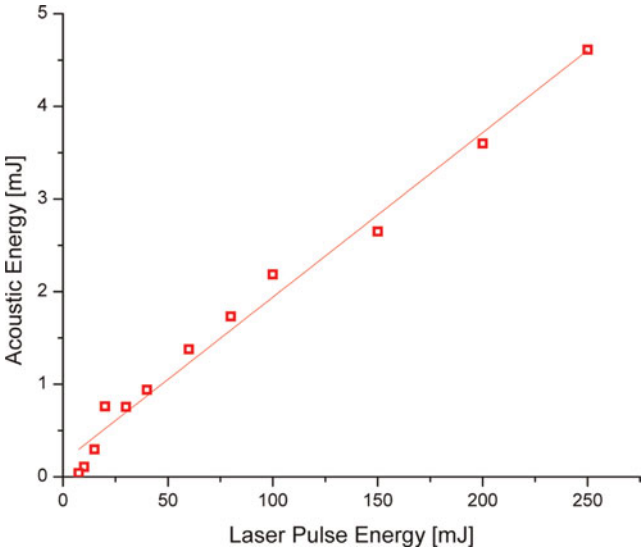


Fig. 14. (Color online) Acoustic energy vs. laser pulse energy. Approximately 2% of the incident laser energy is converted into acoustic energy in the frequency range between 250 Hz and 100 kHz.

4. SUMMARY

In this paper, the results of two experiments, which were made to improve a laser ignition system for internal combustion engines, are presented. This system was developed by the "Laser Ignition Group" at the Vienna University of Technology in cooperation with the GE Jenbacher company.

The minimum laser ignition energy for a methane-air mixture depends on the ignition temperature and the air equivalence ratio. Furthermore, the minimum plasma energy is mainly defined by the ignition pressure and the focal volume.

The investigations on two-color laser ignition covered optical breakdown, plasma absorption efficiency, and plasma scattering for the fundamental wavelength of Nd:YAG and its second harmonic. It turned out that the minimum pulse energy for optical breakdown applying green laser radiation is somewhat lower compared to the breakdown energy of 1064 nm radiation, due to better focusability. Plasma absorption of the infrared light was found to be more important above 10 mJ. It was recognized that plasma transmission losses are much more dominant than scattering losses at both wavelengths. For that reason, further investigations on the plasma characteristics will focus on plasma transmission, considering different focusing parameters. Investigation of acoustic plasma shock waves showed that the acoustic energy depends approximately linearly on laser pulse energy. Conversion efficiency is found to be approximately 2%.

ACKNOWLEDGEMENTS

This project would not have been possible without the support of the Austrian Industrial Development Fund FFG, Project No. 813037, and GE Jenbacher Company, Jenbach, Tyrol, Austria. Furthermore, the authors would like to thank the Austrian Hochschuljubiläumsstiftung for financing under Project No. H-1769/2008.

REFERENCES

Barnes, N.P., Storm, M.E., Cross, P.L. & Skolaut Jr., M.W., (1990). Efficiency of Nd laser materials with laser diode pumping. *IEEE Quan. Electr*. **26**, 558–569.

Bäuerle, D. (2000). *Laser Processing and Chemistry*. Berlin: Springer.

Bradley, D., Sheppard, C.G.W., Suardjaja, I.M. & Wooley, R. (2004). Fundamentals of high-energy spark ignition with lasers. *Combus. Flame* **138**, 55–77.

Dewhurst, R.J. (1982). Quantitative measurements of laser-generated acoustic waveforms *J. Appl. Phys*. **53**, 4064–4071.

Fahy, F. (2001). *Foundation of Engineering Acoustics*. New York: Elsevier.

Glassmann, I. (1987). *Combustion*. New York: Academic Press.

Griem, H.R. (1997). *Principles of Plasma Spectroscopy*. New York: Cambridge University Press.

Gross, S. (2008). *Two-Colour Laser Ignition.* Master Thesis. Vienna: Vienna University of Technology.

Huang, C.C., Shy, S.S., Liu, C.C. & Yan, Y.Y. (2007). A transition on minimum ignition energy for lean turbulent methane combustion in flamelet and distributed regimes. *Proc. Combus. Instit*. **31**, 1401–1409.

Hughes, T.P. (1975). *Plasmas and Laser Light*. New York: Wiley.

Kofler, H. (2005). *Brennraumfenster – eine Schlüsselkomponente der laserinduzierten Zündung von Verbrennungsmotoren*. Diploma Thesis. Vienna: Vienna University of Technology.

Kofler, H., Tauer, J., Iskra, K., Tartar, G. & Wintner, E. (2007). An innovative solid-state laser for engine ignition. *Laser Phys. Lett*. **4**, 322–327.

Kopecek, H. (2004). *Laser Ignition of Gas Engines.* Doctoral Thesis. Vienna: Vienna University of Technology.

Kopecek, H., Wintner, E., Lackner, M., Winter, F. & Hultqvist, A. (2003). Laser-stimulated ignition in a homogeneous charge compression ignition engine. *SAE International SP* **1819**, 183–188.

https://doi.org/10.1017/S0263034609990668 Published online by Cambridge University Press

Lackner, M. (2008). *Laser in Chemistry – Influencing Matter*. New York: Wiley-VCH.

Landau, L.D. & Lifschitz, E.M. (1979). *Physikalische Kinetik*. Berlin: Akademic-Verlag.

Lee, J.H. & Knystautas, R. (1969). Laser spark ignition of chemically reactive gases. *AIAA* **7**, 312–317.

Lewis, B. & Elbe, G.V. (1987). *Combustion, flames and explosions of gases*. New York: Academic Press.

Mastorakos, E. (2009). Ignition of turbulent non-premixed flames. *Progress in Energy and Combustion Science* **35**, 57–97.

Miziolek, A.W., Palleschi, V. & Schechter, I. (2006). Laser-induced breakdown spectroscopy. Fundamentals and Application. New York: Cambridge University Press.

Morgan, C.G. (1975). Laser-induced breakdown of gases. *Rept. Prog. Phys*. **38**, 621–665.

Morgan, C.G. & Ireland, C.M.L. (1973). Gas breakdown by a short laser pulse. *Appl. Phys. D* **6**, 720–730.

Phuoc, T.X. (2000). Laser spark ignition: Experimental determination of laser-induced breakdown of combustion gases. *Opt. Commun*. **175**, 419–423.

Phuoc, T.X. (2003). Laser-induced spark ignition fundamentals and applications. *Opt. Laser Engin*. **44**, 351–397.

Radziemski, L.J. & Cremers, D.A. (1989*a*). *Laser-Induced Plasma and Applications*. New York: Marcel Dekker Inc.

Radziemski, L.J. & Cremers, D.A. (1989*b*). *Laser-Induced Plasmas and Applications*, New York: Marcel Dekker Inc.

Raizer, Y.P. (1991). *Gas Discharge Physics*. Berlin: Springer.

Reider, G. (2004). *Photonik - Eine Einführung in die Grundlagen*. New York: Springer.

Ronney, P.D. (1994). Laser versus conventional ignition of flames. *Opt. Engin*. **33**, 510–521.

Schwarz, E. (2008). *Development and Testing of a Laser for Engine Ignition.* Diploma Thesis. Vienna: Vienna University of Technology.

Sobral, H. (2000). Temporal evolution of the shock wave and hot core air in laser induced plasma. *Appl. Phys. Lett*. **77**, 3158–3160.

Tartar, G., Ranner, H., Winter, F. & Wintner, E. (2008). Simulation of optical breakdown in nitrogen by focused short laser pulses of 1064 nm wavelength. *Laser Part. Beams* **26**, 567–537.

Tauer, J. (2006). *Development of an Ignition Laser.* Diploma Thesis. Vienna: Vienna University of Technology.

Tauer, J., Kofler, H. & Wintner, E. (2010). Laser-initiated ignition. *Laser Photonics Rev*. (In press).

Vogel, A. (1999). Energy balance of optical breakdown in water at nanosecond to femtosecond time scales. *Appl. Phys. B: Laser Opt*. **68**, 271–280.

Weinberg, F.J. & Wilson, J.R. (1971). A Preliminary Investigation of the Use of Focused Laser Beams for Minimum Ignition Energy Studies *Proc. R. Soc. Lond. A* **321**, 41–52.

Weinrotter, M. (2006). *Laser Ignition of Internal Combustion Engines – Basic Laser and Ignition Optics Developments, Engine Application and Optical Diagnostics.* Doctoral Thesis. Vienna: Vienna University of Technology.

Weinrotter, M., Schwecherl, B., Kopecek, H., Wintner, E., Klausner, J. & Herdin, G. (2005). Laser-Ignition of Methane-Air Mixtures at High Pressures and Temperatures *Proceedings of European Combustion Meeting*. Louvain-la-Neuve, Belgium.

Williams, F.A. (1985). *Combustion Theory*. Menlo Park, CA: Benjamin/Cummings Pub.

Yablonovitch, E. (1974). Self-phase modulation and short-pulse generation from laser-breakdown plasmas. *Phys. Rev. A* **10**, 1888.

https://doi.org/10.1017/S0263034609990668 Published online by Cambridge University Press